Optics Communications 286 (2013) 228–232

Contents lists available at SciVerse ScienceDirect

Optics Communications

journal homepage: www.elsevier.com/locate/optcom

Resonant photoluminescence of Si layers grown on SiO_2

A.A. Shklyaev [a,b,*], D.V. Gulyaev [a], K.S. Zhuravlev [a], A.V. Latyshev [a,b], V.A. Armbrister [a], A.V. Dvurechenskii [a]

[a] A.V. Rzhanov Institute of Semiconductor Physics SB RAS, Novosibirsk 630090, Russia
[b] Novosibirsk State University, Novosibirsk 630090, Russia

ARTICLE INFO

Article history:
Received 8 March 2012
Received in revised form
4 August 2012
Accepted 9 September 2012
Available online 24 September 2012

Keywords:
Silicon growth
Silicon-on-insulator
Dislocations
Resonant photoluminescence in 1.5 μm region
Surface morphology

ABSTRACT

The Si layers grown on SiO_2 at temperatures between 430 and 550 °C and annealed at high temperatures emit a photoluminescence (PL) peak in the 1.4–1.7 μm range. The use of 1 nm Ge coverage on SiO_2, prior to the Si deposition, leads to an increase in the PL intensity. The Ge coverage also provides an increase in the average size of microcrystals in Si layers. Thick Si layers (~5 μm) exhibit resonant PL peaks in a broad spectral region from 1.2 to 1.7 μm. The results show that the Si layers prepared on SiO_2 under certain conditions are promising for the fabrication of light emitters on the basis of resonant cavity structures.

1. Introduction

The increase in the luminescence efficiency from crystalline silicon can be achieved through the modification of its electronic structure by creating energy levels in the band gap. In particular, this can be realized by the introduction of dislocations and point defects [1,2]. It has been recently shown that a high concentration of dislocations can be formed during Si growth on the oxidized Si surfaces [3–5]. Dislocations in silicon cause the appearance of four luminescence lines indicated as D1–D4 in the wavelength range 1.2–1.6 μm [1].

The isotropic character of spontaneous luminescence results in its low external quantum efficiency. The increase in the quantum yield of luminescence can be obtained by the creation of conditions for directional emission and for the emission at selective wavelengths. These are usually achieved by the preparation of resonant structures, such as photonic crystal nanocavities on thin layers [6] or distributed Bragg reflector cavities. The layers of silicon on insulator, namely on SiO_2, are required for these purposes. Photonic crystal nanocavities were recently successfully fabricated to produce resonant photoluminescence (PL) peaks in the wavelength range 1.2–1.7 μm using the Si layers containing Ge quantum dots [7–9], Ge layers [10] and commercial silicon-on-isolator structures [11–14]. In the latter case the PL intensity, being measured from the Si layers without nanocavities, was very weak and related to the residual defects. It is suggested that Si layers on SiO_2 which, by themselves, produce an intense PL should be more effective for the fabrication of light emitters with high external quantum efficiency.

It is shown here that the Si layers with an intense PL can be prepared on the surface of SiO_2 films by molecular-beam epitaxy at certain growth and post-growth annealing conditions. The PL properties and the surface morphology are studied for the Si layers with thicknesses ranging from 0.2 to 5 μm as a function of temperatures of growth and post-growth annealing and of the presence of ultra-thin Ge layers (about 1 nm thick) on the SiO_2 surface prior to Si deposition.

2. Experimental details

The 4 in. Si wafers covered with a 1 μm thermal SiO_2 film were used as substrates. The growth was carried out using the molecular beam epitaxy (MBE) system (Riber Siva 21) equipped with electron-beam evaporators for Si and Ge deposition. After the degassing of substrates by heating in the MBE preparation chamber, the Si growth was performed either directly on the surface of SiO_2 films or after the 1 nm Ge deposition. The growth was carried out at various temperatures.

The substrates with the grown layers were cut into samples which were annealed in a dry O_2 atmosphere at different temperatures.

* Corresponding author at : A.V. Rzhanov Institute of Semiconductor Physics SB RAS, Novosibirsk 630090, Russia.
E-mail addresses: alexsan@mail.ru, shklyaev@isp.nsc.ru (A.A. Shklyaev).

0030-4018/$ - see front matter © 2012 Elsevier B.V. All rights reserved.
http://dx.doi.org/10.1016/j.optcom.2012.09.027

Thinning the Si layers was carried out by thermal oxidation and removal of the grown SiO_2 film by etching. The surface morphology of the samples was investigated using the atomic force microscope (AFM) manufactured by NT-MDT. The PL spectra were measured with a standard lock-in technique in conjunction with a Ge detector and a grating monochromator. A Nd:YAG laser operating with the wavelength of 532 nm was used for the PL excitation.

The initial stages of the Si and Ge growth on the surface of tunnel-thin Si oxide films were studied using a scanning tunneling microscope (STM) manufactured by Omicron NanoTechnology. It was equipped with solid sources for the Si and Ge deposition. The Si oxide films were prepared by the exposure of the clean Si surfaces to O_2 at the pressure of 1×10^{-5} Torr at 500 °C in the ultrahigh-vacuum chamber of the STM. These conditions lead to 0.3–0.5 nm Si oxide film formation [15].

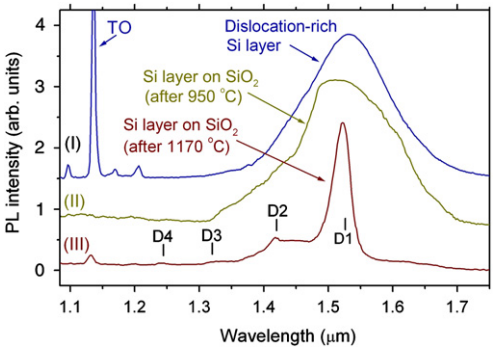

Fig. 1. Low-temperature (5 K) PL spectra of the samples with Si layers: (I) The 100 nm Si layer grown on the oxidized Si surface at 470 °C [16] (the spectrum of this layer is added only for comparison) and the 250 nm Si layers grown on SiO_2 at 500 °C, which were annealed (II) at 950 °C for 30 min and (III) at 1170 °C for 5 min. The 1 nm Ge coverage on SiO_2 was used prior to the Si deposition. The spectra were normalized for the same peak intensity in the 1.5–1.6 μm region.

3. Experimental results and discussion

The Si layers grown on SiO_2 at 500 °C and annealed at 950 °C emit a PL peak centered at 1.5 μm (Fig. 1). Annealing the sample at the higher temperature of 1170 °C leads to a significant narrowing of the PL peak at 1.5 μm and the appearance of a very weak PL of the other dislocation-related D lines. The PL spectrum of the dislocation-rich Si layers is plotted in Fig. 1 for comparison. This Si layer contains dislocations with a concentration of 10^{11}–10^{12} cm^{-2} [4,16], which was prepared by the Si deposition on the oxidized Si surface covered with a dense array of Ge islands. The comparison of the PL spectra shows that they have similar PL properties. The PL spectra also exhibit the PL peaks from indirect interband radiative transitions. The most intense one marked as TO originates from the transverse optical phonon-assisted transitions.

The PL intensity of Si layers grown on SiO_2 was lower than that of the Si layers grown on SiO_2 covered with a 1 nm Ge layer (Fig. 2). The presence of the Ge layer also influences on the size of Si grains in the grown Si layer and on its surface morphology, making the grains larger and more uniform in size. The initial stages of the Si and Ge growth on SiO_2 were studied with STM. In the STM experiments, the deposition was performed on the surface of ultra-thin (~0.5 nm) Si oxide films at the temperature of 430 °C and below. At such low temperatures, the volatile reaction products, that is SiO and GeO molecules, do not form in the interaction of Si or Ge adatoms with the Si oxide film [17] and the growth occurs by the same mechanism as the growth on the surface of thick SiO_2 films. The Ge deposition leads to

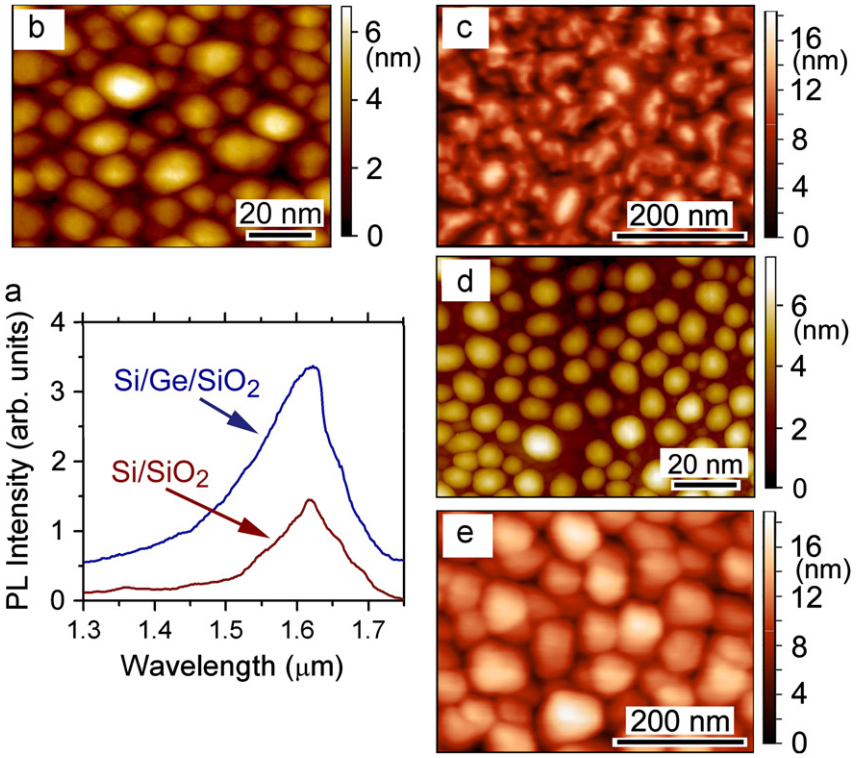

Fig. 2. (a) PL spectra (measured at 80 K) of samples with 250 nm Si layers grown on SiO_2 and on the SiO_2 surface covered with the array of Ge islands. Both samples were being post-grown annealed at 950 °C for 30 min. (b) and (c) STM and AFM images of the surfaces of 3 and 250 nm Si layers deposited on SiO_2 respectively. (d) STM images of the 1 nm Ge layer deposited on SiO_2. (e) AFM image of the 250 nm Si layer deposited on SiO_2 covered with Ge islands. The Si and Ge deposition was carried out at 400 and 430 °C in the STM and AFM cases, respectively.

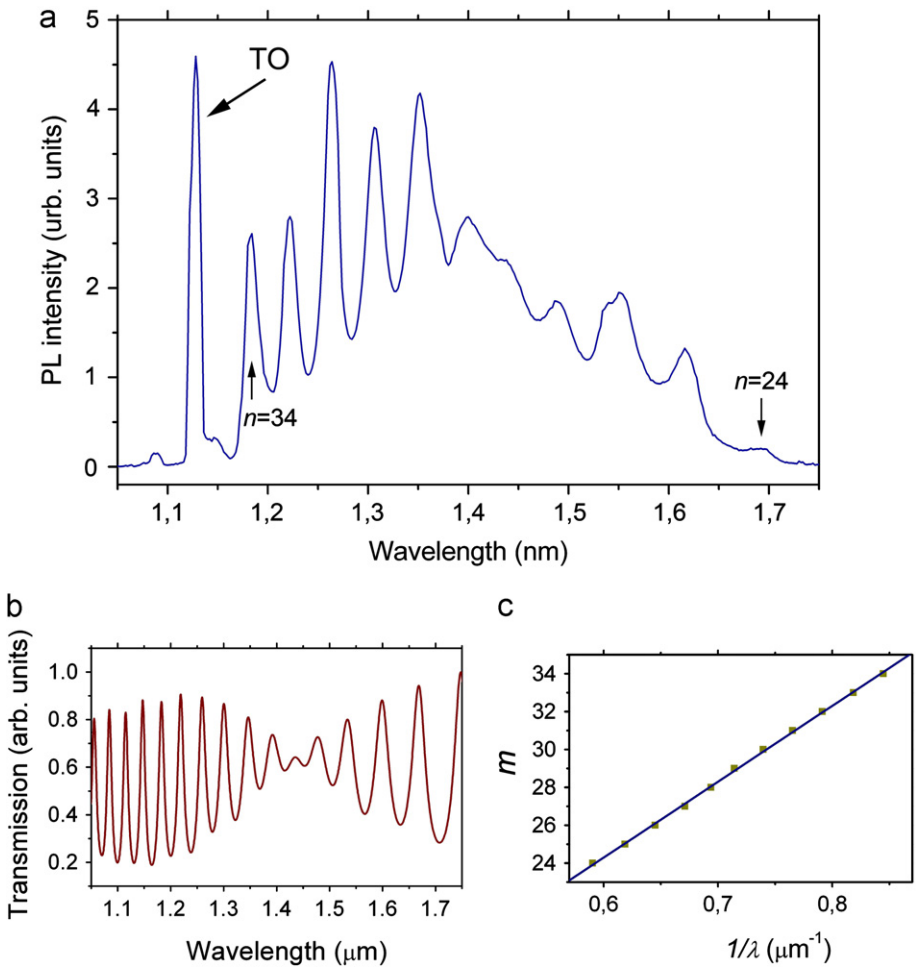

Fig. 3. (a) PL and (b) transmission spectra of the sample with the 5 μm Si layer grown on the 1 μm SiO_2 film covered with an array of Ge islands. The PL spectrum was measured at 5 K. The sample was annealed at 950 °C for 30 min. (c) Number (m) of halves the wavelengths at which the peaks are observed in the spectrum (a) as a function of the inverse wavelengths. The straight line in (c) is the result of fitting Eq. (1) to the experimental data.

the formation of rounded three-dimensional islands with a concentration of $\sim 10^{12}$ cm^{-2} [Fig. 2(d)]. The similar dense arrays of Ge islands were observed previously [17–19]. The round-shaped islands are also formed when Si is deposited on the oxidized Si surface at low temperatures [Fig. 2(b)] [20,21]. Round-shaped areas in the surface morphology remain, during the subsequent Si depositions, on both types of the surfaces (covered or not with the Ge islands) [Fig. 2(c) and (e)].

It has been recently shown that the rounded shape of the surface areas of grown Si layers is the result of the presence of threading dislocations. Crystal growth occurs by the attachment of adatoms to the edges of atomic steps. Atomic steps usually appear as a result of nucleation of new two-dimensional layers on atomically flat terraces. Another source of the atomic steps is threading dislocations. Due to the existence of a high kinetic barrier for the new layer nucleation, the surface morphology is usually composed of large flat terraces. The lack of such terraces suggests that there are permanent sources of the atomic steps which are threading dislocations [22]. Thus, the round-shaped surface morphology is the result of the presence of a high concentration of threading dislocations in the grown Si layers.

The concentration of excited carriers in silicon is governed by the balance between the rates of carrier excitation and nonradiative recombination [5]. The stronger PL intensity from the Si layers grown on SiO_2 covered with Ge islands [Fig. 2(a)] suggests that they are characterized by the lower nonradiative recombination rate in comparison with that of the Si layers grown directly on SiO_2. These can be the result of better crystalline quality of the Si layers grown using Ge islands due to their larger sizes of crystalline grains.

The PL spectra of the thick Si layers exhibit a series of peaks separated by approximately 30 meV [Fig. 3(a)]. Since the grown Si layer is located between two light-reflecting interfaces, namely the Si/SiO_2 and Si/air, the PL peaks are the result of luminescence interference. The peak positions in the PL spectra are correlated with the features of the transmission spectrum of the sample [Fig. 3(b)]. The enhancement of the luminescence occurs at the following relationship between the thickness L of the layer and the wavelength λ_{vac} of the luminescence in the vacuum [23]

$$2\pi nL/\lambda_{vac}+\psi = 2m\pi \quad (m = 1,2,3,\ldots) \tag{1}$$

where n is the refractive index of the Si layer for λ_{vac} and ψ, denotes the phase shifts corresponding to the light redistribution due to reflection and absorption by the interfaces. The position of peaks in the PL spectrum is well described by Eq. (1), as shown in Fig. 3(c). In accordance with the transmission spectrum, the lack of well pronounced peaks in the wavelength range of 1.4 μm is the result of the action of other light reflecting interface, namely the SiO_2-film/Si-substrate.

The PL intensity of the sample decreased with the increasing temperature, as shown in Fig. 4, and almost disappeared at temperatures above 200 K. During the experiment, the sample temperature was variable while other conditions were fixed. The temperature dependence indicates that the peaks in the PL

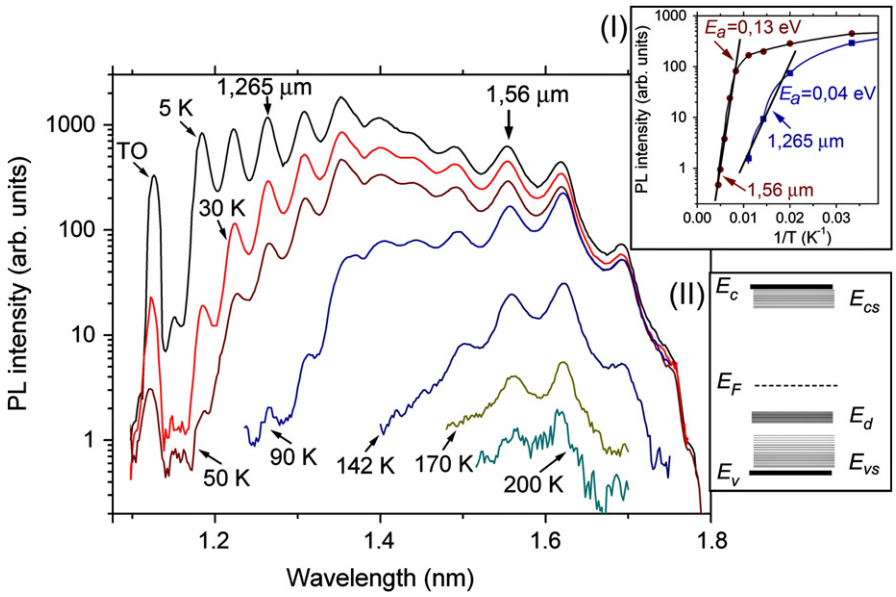

Fig. 4. PL spectra at different temperatures of the sample which was prepared at the same conditions as the sample used for Fig. 3. The decrease of the PL intensity at wavelengths greater than 1.7 μm is due to the detector cutoff. Inset (I) shows the dependence of the PL intensity on the inverse temperature for two wavelengths of 1.265 and 1.56 μm. The curves represent the approximation of experimental data by Eq. (2). Inset (II) shows the scheme of energy levels (described in the text) that are involved into the radiative transitions in the grown Si layers.

spectra originate from the interference of PL emitted by the grown Si layers.

The PL of thick Si layers is observed in a broad spectral range approximately between 1.2 and 1.8 μm [Figs. 3(a) and 4]. The observation of PL in the short wavelength region indicates the appearance of radiative transitions occurring through shallow bands E_{cs} and E_{vs} located near the conduction and valence band edges, respectively. The existence of the shallow bands in dislocated Si is well known from the theoretical and experimental studies [24–27]. However, radiative transitions between the dislocation-related shallow bands have not been previously observed from the grown Si layers [16]. These radiative transitions could be enhanced due to the presence of the light-reflecting interfaces. Such an effect was observed from the crystalline Si layer on SiO_2 after changing the light-reflecting conditions by the formation of photonic crystals [14].

The decrease in PL intensity with an increasing temperature starts in the region of short wavelengths, which is related to radiative transitions through the shallow levels (Fig. 4). The temperature dependence of PL intensity, I_{PL} can be written in the form of

$$I_{PL} = I_{PL}^{(o)}/[1+\sum_i A_i \exp(-E_i/kT)] \quad (i=1,2) \qquad (2)$$

where $I_{PL}^{(o)}$ and A_i are the numerical coefficients and E_i are the activation energies. The results of fitting Eq. (2) to the experimental data are shown in Fig. 4 [Inset (I)]. The activation energies of 0.004 and 0.04 eV describe the temperature dependence measured for the relatively short wavelength of 1.265 μm. The latter value characterizes the temperature-induced changes in the excess carrier populations in the shallow bands. The PL in the long-wavelength region is related to electronic transitions through the deep levels. The rapid temperature-induced decrease in PL intensity measured at 1.56 μm is characterized by the activation energy $E_F - E_d = 0.13$ eV, where E_F is the Fermi level and E_d is the energy of the deep level band [28]. Since the optically active deep states are located at 0.3–0.4 eV above the valence band edge [29], this gives the position of the Fermi level close to the middle of the Si band gap, as shown in inset (II) in Fig. 4, where E_c and E_v are the levels of conduction and valence band edges. This Fermi level position is quite expectable for our non-doped Si layers.

Annealing the samples with the grown Si layers at high temperatures from 950 to 1100 °C in an O_2 atmosphere results in the increase in the PL intensity by one order of magnitude, as shown in Fig. 5 (a). The increase in the PL intensity could occur for two reasons. As the Si layers are grown on SiO_2 at relatively low temperatures, they contain a high concentration of crystal defects acting as nonradiative recombination centers. The high-temperature annealing usually leads to a decrease in the defects concentration [13]. The other reason can be related to the surface roughness of the Si layers which can reduce the external quantum yield of the PL. The study of the surface morphology by AFM has shown that the thermal oxidation of the samples and the subsequent removal of the SiO_2 film from the sample surface lead to a decrease in surface roughness. The intensity of the resonant PL peaks is enhanced for such samples, as shown in Fig. 5 (b). However, this does not significantly affect the temperature dependence of the PL intensity.

The intense resonant PL peaks from the photonic crystal nanocavities with different topologies have been recently obtained at room temperature. This was achieved for commercial Si layers on SiO_2 [14], as well as for the Si layers containing Ge quantum dots [7–9]. The comparison has shown that the dislocation-rich Si layers grown on the oxidized Si surfaces produce the PL that is more intense than the PL from the Si layers with Ge quantum dots [3]. It is shown here that the dislocation-rich Si layers can be fabricated by the direct Si deposition on SiO_2 or on the SiO_2 surface covered with the ultrathin Ge layer. Such grown Si layers can be annealed at temperatures up to 1170 °C, which leads even to an increase in PL intensity. The ability to conduct the high-temperature annealing allows fabricating the resonant light emitters using conventional processes of the Si technology and, thereby, it gives an opportunity for the monolithic optoelectronic device preparation in a uniform process.

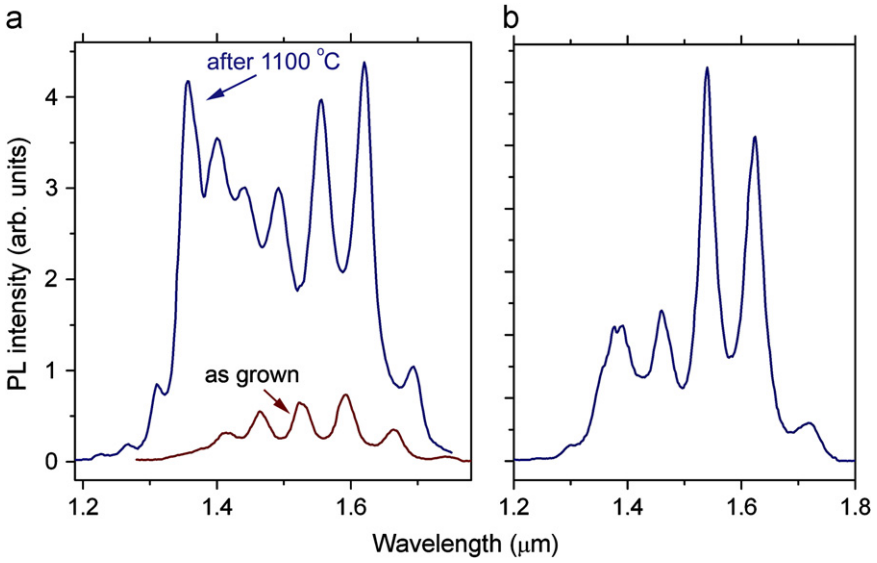

Fig. 5. PL spectra of the samples with the 5 μm Si layer (a) before and after annealing at 1100 °C for 5 min, (b) after annealing in an O_2 atmosphere for 3 h at 1100 °C and subsequent removal of the thermal SiO_2 film from the sample surface. The PL spectra were measured at 80 K.

4. Conclusion

The Si layers grown on SiO_2 at temperatures from 430 to 550 °C and annealed at 900–1100 °C exhibit a PL peak centered at 1.5–1.6 μm. The deposition of a 1 nm Ge layer on the SiO_2 surface prior to the Si growth leads to an increase in the PL intensity. The use of the Ge layer also improves the uniformity of surface morphology of the Si layer. The round-shaped areas observed in the surface morphology are caused by threading dislocations. The presence of light reflecting interfaces from the both sides of the Si layer creates conditions for the resonant PL producing the multiple peaks in the broad wavelength region from 1.2 to 1.7 μm. The long-time annealing of the samples at 1100 °C in O_2 atmosphere causes the enhancement in the PL intensity of the resonant peaks in the wavelength range 1.5–1.6 μm. This observation shows that the Si layers grown on SiO_2 are suitable for the preparation of photonic crystal or distributed Bragg reflector cavities.

Acknowledgments

This study is partially supported by the Russian Foundation for Basic Research (Project no. 11-07-00475-a) and the RAS Presidium Program (Grant no. 24.21).

References

[1] N.A. Drozdov, A.A. Patrin, V.D. Tkachev, JETP Letters 23 (1976) 597.
[2] E.Ö. Sveinbjörnsson, J. Weber, Applied Physics Letters 69 (1996) 2686.
[3] A.A. Shklyaev, S. Nobuki, S. Uchida, Y. Nakamura, M. Ichikawa, Applied Physics Letters 88 (2006) 121919.
[4] A.A. Shklyaev, M. Ichikawa, Physics Uspekhi 51 (2008) 133.
[5] A.A. Shklyaev, F.N. Dultsev, K.P. Mogilnikov, A.V. Latyshev, M. Ichikawa, Journal of Physics D: Applied Physics 44 (2011) 025402.
[6] A.B. Matsko (Ed.), Practical Applications of Microresonators in Optics and Photonics, CRC Press, Taylor and Francis Group, Boca Raton, 2009 553 p.
[7] X. Li, P. Boucaud, X. Checoury, O. Kermarrec, Y. Campidelli, D. Bensahel, Journal of Applied Physics 99 (2006) 023103.
[8] J. Xia, Y. Takeda, N. Usami, T. Maruizumi, Y. Shiraki, Optics Express 18 (2010) 13945.
[9] N. Hauke, S. Lichtmannecker, T. Zabel, F.P. Laussy, A. Laucht, M. Kaniber, D. Bougeard, G. Abstreiter, J.J. Finley, Y. Arakawa, Physical Review B 84 (2011) 085320.
[10] M. El Kurdi, S. David, X. Checoury, G. Fishman, P. Boucaud, O. Kermarrec, D. Bensahel, B. Ghyselen, Optics Communications 281 (2008) 846.
[11] Y. Akahane, T. Asano, B.S. Song, S. Noda, Nature 425 (2003) 944.
[12] M. Fujita, Y. Tanaka, S. Noda, IEEE Journal of Selected Topics in Quantum Electronics 14 (2008) 1090.
[13] J. Wang, Y. Song, W. Yan, M. Qiu, Optics Communications 283 (2010) 2461.
[14] R. Lo Savio, S.L. Portalupi, D. Gerace, A. Shakoor, T.F. Krauss, L. O'Faolain, L.C. Andreani, M. Galli1, Applied Physics Letters 98 (2011) 201106.
[15] T. Yasuda, S. Yamasaki, M. Nishizawa, N. Miyata, A. Shklyaev, M. Ichikawa, T. Matsudo, T. Ohta, Physical Review Letters 87 (2001) 037403.
[16] A.A. Shklyaev, S.P. Cho, Y. Nakamura, N. Tanaka, M. Ichikawa, Journal of Physics: Condensed Matter 19 (2007) 136004.
[17] A.A. Shklyaev, M. Shibata, M. Ichikawa, Physical Review B 62 (2000) 1540.
[18] A.I. Nikiforov, V.V. Ul'yanov, O.P. Pchelyakov, S.A. Teys, A.K. Gutakovsky, Physics of the Solid State 47 (1) (2005) 67.
[19] L. Zhang, H. Ye, Y.R. Huangfu, C. Zhang, X. Liu, Applied Surface Science 256 (2009) 768.
[20] A.A. Shklyaev, M. Ichikawa, Physical Review B 65 (2002) 045307.
[21] A.A. Saranin, A.V. Zotov, V.G. Kotlyar, O.A. Utas, K.V. Ignatovich, T.V. Kasyanova, Y.S. Park, W.J. Park, Applied Surface Science 243 (2005) 199.
[22] A.A. Shklyaev, K.N. Romanyuk, A.V. Latyashev, A.V. Arzhannikov, JETP Letters 94 (2011) 477.
[23] I.E. Tyschenko, K.S. Zhuravlev, A.G. Cherkov, V.P. Popov, A. Misiuk, R.A. Yankov, Applied Physics Letters 89 (2006) 013106.
[24] F. Liu, M. Mostoller, V. Milman, M.F. Chisholm, T. Kaplan, Physical Review B 51 (1995) 17192.
[25] N. Lehto, Physical Review B 55 (1997) 15601.
[26] Yu.S. Lelikov, Yu.T. Rebane, S. Ruvimov, A.A. Sitnikov, D.V. Tarhin, Yu.G. Shreter, Physica Status Solidi B: Basic Solid State Physics 172 (1992) 53.
[27] V. Kveder, T. Sekiguchi, K. Sumino, Physical Review B 51 (1995) 16721.
[28] W. Shockley, W.T. Read, Physical Review 87 (1952) 835.
[29] A.T. Blumenau, R. Jones, S. Oberg, P.R. Briddon, T. Frauenheim, Physical Review Letters 87 (2001) 187404.